# Carboxymethylated Liver Alcohol Dehydrogenase: Kinetic and Thermodynamic Characterization of Reactions with Substrates and Inhibitors†

Knut H. Dahl‡ and Michael F. Dunn*

ABSTRACT: Liver alcohol dehydrogenase (LADH) carboxymethylated at Cys-46 (CMLADH) forms two different ternary complexes with 4-*trans*-(*N*,*N*-dimethylamino)cinnamaldehyde (DACA). The complex with reduced nicotinamide adenine dinucleotide (NADH) is characterized by a 38-nm red shift of the long-wavelength $\pi,\pi^*$ transition to 436 nm, while the complex with oxidized nicotinamide adenine dinucleotide ($NAD^+$) is characterized by a 60-nm red shift to 458 nm. CMLADH also forms a ternary complex with $NAD^+$ and the *Z* isomer of 4-*trans*-(*N*,*N*-dimethylamino)cinnamaldoxime in which the absorption of the oxime ($\lambda_{max}$ = 354 nm) is red shifted 80 nm to 434 nm. Pyrazole and 4-methylpyrazole are weak competitive inhibitors of ligand binding to the substrate site of native LADH. These inhibitors were found to form ternary complexes with CMLADH and NADH which are more stable than the corresponding complexes with the native enzyme. The transient reductions of the aldehydes DACA and *p*-nitrobenzaldehyde (NBZA) were studied under single-turnover conditions. Carboxymethylation decreases the DACA reduction rate 80-fold and renders the process essentially independent of pH over the region 5–9, whereas this process depends on a p$K_a$ of 6.0 in the native enzyme. At pH 7.0, the rate constant for NBZA reduction also is decreased at least 80-fold to a value of 7.7 ± 0.3 $s^{-1}$. Since primary kinetic isotope effects are observed when NADH is substituted with (4*R*)-4-deuterio-NADH ($k_H/k_D$ = 3.0 for DACA and $k_H/k_D$ = 2.3 for NBZA), the rate-limiting step for both aldehydes involves hydride transfer. The altered pH dependence is concluded to be due to an increase in the p*K* value of the zinc-coordinated DACA–alcohol in the ternary complex with $NAD^+$ by more than 3 units. This perturbation is brought about by the close proximity of the negatively charged carboxymethyl carboxylate.

Iodoacetate reacts with liver alcohol dehydrogenase (LADH, EC 1.1.1.1)[1] by preferentially carboxymethylating Cys-46 (Harris, 1964; Li & Vallee, 1964), one of the three protein ligands to the active-site zinc atom (Eklund et al., 1976). Due to the formation of a reversible enzyme–iodoacetate complex prior to the irreversible alkylation of the zinc thiol of Cys-46 (Reynolds & McKinley-McKee, 1969; Dahl & McKinley-McKee, 1981a,b), the reaction is a highly specific, site-directed process.

Reynolds & McKinley-McKee (1975) showed that the modified enzyme retains a small, residual activity in the oxidation of ethanol at neutral pH. At high pH, the aldehyde reducing activity was found to be even higher than for the native enzyme. They also reported that alkylation weakened ternary complexes involving $NAD^+$ and certain aldehydes and inhibitors. X-ray crystallography at a resolution of 0.45 nm showed no major change of the protein structure upon carboxymethylation; the thioether sulfur of carboxymethylated Cys-46 is still ligated to the active-site metal, and the introduced carboxyl group is oriented in the direction of Arg-369 (Zeppezauer et al., 1975). A $^{13}C$ NMR study of enzyme carboxymethylated with bromo[$^{13}C$]acetate has also been performed (Khalifah & Sutherland, 1979; Jones & Khalifah, 1980).

In addition to the original steady-state kinetic studies of alcohol oxidation and aldehyde reduction with CMLADH (Reynolds & McKinley-McKee, 1975), Hardman (1976) has studied the transient kinetics of alcohol oxidation and of NADH binding and dissociation. He concluded that alcohol oxidation is limited by a hydride transfer rate which is 700-fold slower in comparison to the native enzyme. However, thus far no transient kinetic study of aldehyde reduction with the carboxymethylated enzyme has been presented which could explain the remarkable accelerating effect of carboxymethylation on the steady-state rate of aldehyde reduction at high pH.

The mechanism of aldehyde reduction by native LADH as well as by enzyme modified by replacement of the active-site zinc ion with other metals has been extensively studied by transient kinetics using the chromophoric substrate 4-*trans*-(*N*,*N*-dimethylamino)cinnamaldehyde (DACA) (Dunn & Hutchison, 1973; Dunn et al., 1975, 1982; Angelis et al., 1977; Dietrich et al., 1979; Morris et al., 1980). The reduction of this aldehyde is characterized by formation and decay of an intermediate E(NADH,DACA) complex where the $\pi,\pi^*$ electronic transition of the aldehyde chromophore ($\lambda_{max}$ = 398 nm) is red shifted upon complex formation by from 59 to 80 nm, depending on the type of active-site metal. Recently it has also been shown that the native enzyme forms an E-($NAD^+$,DACA) complex in which the DACA absorption is red shifted by 97 nm (Dahl & Dunn, 1984).

The aim of the present work is to determine how carboxymethylation affects the catalytic potential of the enzyme by

† From the Department of Biochemistry, University of California, Riverside, California 92521. *Received April 13, 1984.* This work was supported by NATO Science Fellowship 2822 (awarded to K.H.D.) and National Science Foundation Grant PCM-8108862.

‡ Present address: Nyegaard and Co., Torshov, Oslo 4, Norway.

[1] Abbreviations: LADH, horse liver alcohol dehydrogenase; CME or CMLADH, Cys-46 carboxymethylated horse liver alcohol dehydrogenase; $NAD^+$ and NADH, oxidized and reduced nicotinamide adenine dinucleotide, respectively; NADD, (4*R*)-4-deuterio-NADH; alc, alcohol; ald, aldehyde; DACA, 4-*trans*-(*N*,*N*-dimethylamino)cinnamaldehyde; DMOX, 4-*trans*-(*N*,*N*-dimethylamino)cinnamaldoxime; NBZA, *p*-nitrobenzaldehyde; pyr, pyrazole; Me-pyr, 4-methylpyrazole; TFE, 2,2,2-trifluoroethanol; MES, 2-(*N*-morpholino)ethanesulfonic acid; TES, *N*-[tris(hydroxymethyl)methyl]-2-aminoethanesulfonic acid; TAPS, 3-[[tris(hydroxymethyl)methyl]amino]propanesulfonic acid; ADPR, adenine diphosphoribosyl.

0006-2960/84/0423-6829$01.50/0 

undertaking transient kinetic studies of the reduction both of DACA and of *p*-nitrobenzaldehyde (NBZA). It will be shown that DACA forms ternary complexes with both CME($NAD^+$) and CME($NAD^+$) in which the carbonyl oxygen of DACA is directly coordinated to the active-site zinc. To further compare the properties of native and carboxymethylated LADH, we have investigated the binding of a variety of LADH ligands to CME and to CME(coenzyme) complexes.

## Experimental Procedures

*Materials.* To keep the buffers free of anions which inhibit coenzyme binding, buffers of MES, TES, and TAPS were prepared with doubly glass-distilled water from the free acids by adding NaOH to the desired pH (Dahl & McKinley-McKee, 1981a,b; Dietrich et al., 1983). LADH was obtained from Boehringer Mannheim and prior to use was first dialyzed extensively against phosphate buffer, pH 7.0, and then freed from phosphate by dialysis against two changes of 25 mM TES/$Na^+$, pH 7.0.

The coenzymes $NAD^+$ and NADH were purchased from Sigma Chemical Co. as grade III. DACA, pyrazole, and isobutyramide were obtained from Aldrich. The *Z* isomer of DMOX was synthesized according to Abdallah et al. (1984). Iodoacetic acid and 4-methylpyrazole were obtained from Sigma Chemical Co. Decanoic acid, trifluoroethanol, imidazole, and NBZA were obtained from Aldrich Chemical Co. DACA, pyrazole, and NBZA were purified by vacuum sublimation while isobutyramide and iodoacetic acid were recrystallized from water.

*Preparation and Assay of CMLADH.* LADH was carboxymethylated at 25 °C with iodoacetate (2 mM) in 25 mM TES/$Na^+$ buffer, pH 7.0, in the presence of imidazole (10 mM) to increase the rate and specificity of Cys-46 alkylation (Evans & Rabin, 1968; Reynolds et al., 1970; Dahl & McKinley-McKee, 1981b). The reaction went on for about 3 h (>25 half-lives for the alkylation). The carboxymethylated enzyme was then dialyzed against the same buffer to remove excess iodoacetate and imidazole. The LADH concentration during alkylation ranged from 100 to 230 $\mu$M (depending on the preparation). The specific activity for the native enzyme (Dalziel, 1957) was normally 14–16 $\Delta A_{340}$ $min^{-1}$ $mg^{-1}$, while the specific activity of eight different CMLADH preparations was 0.30 ± 0.05 $\Delta A_{340}$ $min^{-1}$ $mg^{-1}$. In agreement with previous studies (Reynolds & McKinley-McKee, 1975), this value corresponds to 2% of the native enzyme.

Differences in the fluorescence properties of CME(NADH) and native E(NADH) provide a sensitive assay for CMLADH (Winer & Theorell, 1960; Reynolds & McKinley-McKee, 1975). Isobutyramide gives a 3-fold increase in the fluorescence emission of native E(NADH) at 410 nm ($\lambda_{ex}$ = 330 nm), while isobutyramide has no effect on the fluorescence of the CME(NADH) complex. CMLADH was also assayed by protein 280-nm absorption using $A^{0.1\%}_{280nm}$ = 0.455 $mg^{-1}$ $cm^2$, the same value as for the native enzyme (Dalziel, 1957). As judged from the above assays, the CMLADH prepared was a homogeneous enzyme virtually free of native enzyme.

*Preparation of NADD and NADH.* The specifically labeled (4*R*)-4-deuterio-NADH (NADD) and isotopically normal NADH used in the deuterium kinetic isotope studies were prepared enzymatically as previously described (Rafter & Colowick, 1957; Dunn & Hutchison, 1973) and further purified by the method of Silverstein (1965).

*Instrumentation.* Static UV–visible spectra were obtained by using a Hewlett Packard 8450A spectrophotometer equipped with cuvette holders thermostated at 25.0 ± 0.2 °C. A Farrand Model M-II spectrofluorometer was used for fluorescence titrations. Single-wavelength transient kinetic studies were caried out on a computerized Durrum-Gibson Model D-110 stopped-flow spectrophotometer interfaced for on-line computer data acquisition and analysis as described previously (Dunn et al., 1979). Rapid-scanning stopped-flow spectrophotometry was carried out on a hybrid instrument consisting of a Durrum Model D-110 Kel-F flow system and a Princeton Applied Research (PAR) OMA-2 multichannel analyzer as described elsewhere (Koerber & Dunn, 1981; Koerber et al., 1983). All stopped-flow studies were carried out at room temperature (25 ± 2 °C).

*Analysis of Titration Data.* The titration data were analyzed by loading the derivative-free nonlinear regression program BMDPAR (Copyright 1981, Regents of University of California) with a function describing the titration curve. The function was developed for the case of titration of enzyme (E) with NADH (R), forming the more fluorescent ER complex.

$$K = \frac{[E_f][R_f]}{[ER]}$$

$$[E_f] = [E_t] - [ER]$$

$$[R_f] = [R_t] - [ER]$$

Here $K$ is the dissociation constant for the ER complex, and the subscripts t and f refer to the total and free concentrations, respectively. Since both ER and R are fluorescent, the observed fluorescence ($F$) is

$$F = f_R[R_f] + f_{ER}[ER]$$

where $f_F$ and $f_{ER}$ are the relative fluorescence coefficients for R and ER, respectively. From these equations, the observed fluorescence can be expressed as a function of $K$, $[E_t]$, $[R_t]$, $f_r$, and $f_{ER}$ as follows:

$$F = f_R\{[R_t] - (a/2) - (a^2 - 4[E_t][R_t])/2\} + f_{ER}\{(a/2) - (a^2 - 4[E_t][R_t])/2\}$$

where $a = [R_t] + [E_t] + K$. Using $F$ and $[R_t]$ as variables allows the determination of the parameters $K$, $f_R$, $f_{ER}$, and $[E_t]$ and their standard deviations. This function can also be generalized to describe spectrophotometric titrations by substituting the relative fluorescence coefficient $f$ with the extinction coefficient $\epsilon$. The BMDPAR program permits one or more of the parameters to be kept constant during the iteration. For the cases where the compound used for titration had no fluorescence or absorption, the fluorescence or extinction coefficient for this species was defined as zero. For the cases where $K \gg [E_t]$, the $[E_t]$ value (e.g., the titration end point) could not be computed, and $[E_t]$ was assigned a value determined via other methods.

## Results

*Properties of CME($NAD^+$).* (*A*) *CME($NAD^+$,pyr) Complex.* Reynolds & McKinley-McKee (1975) in their study of CMLADH reported that titrations with pyrazole in the presence of excess $NAD^+$ showed that the CME($NAD^+$) and the E($NAD^+$) complexes (also designated as CMEO and as EO, respectively) have similar affinities for pyrazole, and this was confirmed in our titrations. At pH 7.0, $K_{EO,pyr}$ has been estimated to be 0.14 $\mu$M (Andersson et al., 1981).

(*B*) *CME($NAD^+$,TFE) Complex.* With native LADH, trifluoroethanol (TFE), a nonreactive alcohol, is a strong inhibitor of the enzyme (Shore et al., 1974; Kvassman & Petersson, 1980a). Inhibition is due to the pH-dependent formation of an E($NAD^+$,TFE) complex with $K_{EO,TFE}$ = 4 $\mu$M.

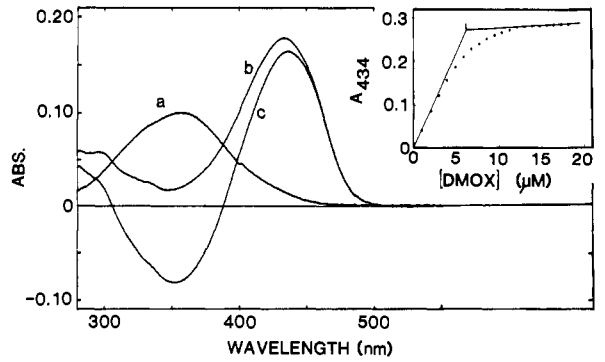


FIGURE 1: Spectra and difference spectrum of the ternary complex formed in the reaction of (*Z*)-DMOX with $NAD^+$ and CMLADH: (a) free (*Z*)-DMOX; (b) spectrum of the CME[$NAD^+$,(*Z*)-DMOX] complex; (c) difference spectrum of (b) − (a). The spectra were recorded as follows: The sample cuvette was a split cuvette with a light path of 2 × 0.438 cm. It contained 10 μN CMLADH in compartment A and 100 μM $NAD^+$ in compartment B. Both compartments contained 0.05 M pyrophosphate buffer, pH 8.75, and all concentrations given are those after mixing. After the spectrophotometer was balanced against a cuvette with water and the base line was recorded, 10 μL of (*Z*)-DMOX was added to compartment A to give a concentration of 5 μM. After (*Z*)-DMOX was added, compartments A and B contained the same volume of solution. Spectrum a, the spectrum of free (*Z*)-DMOX, was then recorded. Mixing compartments A and B immediately gave spectrum b, the CME[$NAD^+$,(*Z*)-DMOX] complex. Subtraction of spectrum a from spectrum b gave the difference spectrum c. Inset: Titration of CMLADH with (*Z*)-DMOX in the presence of excess $NAD^+$. The absorbance change due to formation of CME[$NAD^+$,(*Z*)-DMOX] was measured at 434 nm. Aliquots (10 μL) of a concentrated (*Z*)-DMOX solution were titrated into a cuvette containing 8 μN CMLADH (based on $A^{1\%}_{280nm}$ = 0.455) and 100 μM $NAD^+$ in 0.05 M pyrophosphate buffer, pH 8.75 (total volume was 1 mL). The absorbance has been corrected for dilution during the titration. Nonlinear regression analysis gave a site concentration of 6.1 ± 0.1 μN and a dissociation constant, $K_{CMEO,DMOX}$, of 0.71 ± 0.05 μM.

In the present work, we were unable to find a similar complex with CMLADH. Even in the presence of 0.2 M trifluoroethanol, the steady-state reduction of DACA at pH 7.0 with CMLADH was inhibited only about 50%. Thus, CMLADH and LADH have quite different properties with respect to inhibition by TFE.

(*C*) *CME[NAD⁺,(Z)-DMOX] Complex.* The reaction of 4-*trans*-(*N*,*N*-dimethylamino)cinnamaldoxime (DMOX) with LADH has been studied by Sigman et al. (1982) using a DMOX preparation which may have contained both the *Z* and *E* isomers, whereas Abdallah et al. (1984) showed that the reaction with the enzyme was specific for the *Z* isomer of the oxime. Upon binding to the E($NAD^+$) complex, the $\lambda_{max}$ of the (*Z*)-DMOX chromophore is red shifted from 354 nm in $H_2O$ to 428 nm.

A similar shift of the (*Z*)-DMOX absorption was observed also upon binding to the CME($NAD^+$) complex. Figure 1 shows the spectrum of free (*Z*)-DMOX ($\lambda_{max}$ = 354 nm, $\epsilon_{354}$ = 2.42 × $10^4$ $M^{-1}$ $cm^{-1}$; Abdallah et al., 1984) compared to that of the CME[$NAD^+$,(*Z*)-DMOX] complex ($\lambda_{max}$ = 434 nm, $\epsilon_{434}$ = 4.08 × $10^4$ $M^{-1}$ $cm^{-1}$).

Titration of CME with (*Z*)-DMOX in the presence of excess $NAD^+$ at pH 8.75 (insert to Figure 1) gave a stoichiometry of 0.75 molecule of (*Z*)-DMOX bound per active site (indicating the presence of 25% inactive CME) and a dissociation constant $K_{CMEO,DMOX}$ of 0.71 ± 0.05 μM. This value indicates that DMOX binding is weaker to CME($NAD^+$) than to E($NAD^+$) for which a dissociation constant of 0.01 μM was estimated (Abdallah et al., 1984). We were unable to detect any CME[NADH,(*Z*)-DMOX] complex via changes in the spectrum of the (*Z*)-DMOX chromophore.

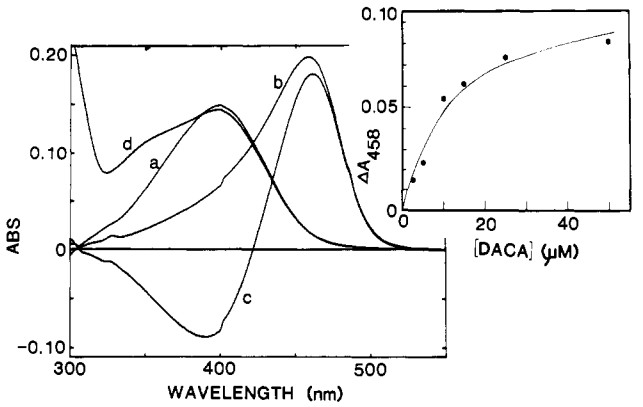


FIGURE 2: Spectra and difference spectrum measured for the reaction of DACA with CME($NAD^+$): (a) free DACA; (b) CME($NAD^+$,DACA); (c) difference spectrum of (b) − (a); (d) final spectrum after addition of pyrazole to CME($NAD^+$,DACA). The spectra were recorded as described in Figure 1. Final concentrations were 30 μN CMLADH, 2 mM $NAD^+$, 5 μM DACA, 8.3 mM pyrazole, and 0.05 M TES/$Na^+$ buffer, pH 7.0, 25.0 ± 0.2 °C. Inset: Formation of CME($NAD^+$,DACA) as a function of the DACA concentration at pH 7.0. Measurements were carried out by rapid mixing in a stopped-flow instrument. Conditions were as follows: for syringe A, 2.5 μN CMLADH in 0.05 M TES/$Na^+$ buffer, pH 7.0; for syringe B, DACA concentration varied, 2 mM $NAD^+$ in the same buffer. The absorbance was read at 458 nm 2 s after flow stopped, and the readings have been corrected for the absorption of free DACA. The dissociation constant for DACA binding to CME($NAD^+$), $K_{CMEO,DACA}$, was calculated to be 9.7 ± 2.2 μM by nonlinear regression.

(*D*) *CME(NAD⁺,DACA) Complex.* When CMLADH, $NAD^+$, and DACA were mixed at pH 7.0, the formation of a CME($NAD^+$,DACA) complex is evidenced by the appearance of a new spectral band with $\lambda_{max}$ = 458 nm (Figure 2). On DACA binding to CME($NAD^+$), the absorption of the free chromophore ($\lambda_{max}$ = 398 nm, $\epsilon_{398}$ = 3.10 × $10^4$ $M^{-1}$ $cm^{-1}$; Dunn & Hutchison, 1973) is red shifted to 458 nm, and the extinction coefficient for this new complex is $\epsilon_{458} \simeq 7.2 \times 10^4$ $M^{-1}$ $cm^{-1}$.

The addition of pyrazole to the CME($NAD^+$,DACA) complex gave spectrum d in Figure 2. It is evident here that the 458-nm band disappears while the peak corresponding to free DACA is quantitatively regained. This experiment shows that pyrazole displaces DACA from the CME($NAD^+$,DACA) complex as the stable CME(NAD–pyr) adduct is formed.

(*E*) *Stability of the CME(NAD⁺,DACA) Complex.* To determine the equilibrium constant for the dissociation of DACA from the CME($NAD^+$,DACA) complex ($K_{CMEO,DACA}$), CME was mixed with $NAD^+$ and increasing amounts of DACA. In this experiment, the rapid-mixing stopped-flow technique was used to follow the appearance of the CME($NAD^+$,DACA) complex at 458 nm. The binding isotherm (inset to Figure 2) was determined from the amplitude of the absorbance changes at 458 nm. It is clear that the binding of DACA to the CME($NAD^+$) complex is subject to a saturation effect. With the use of a nonlinear regression, the apparent dissociation constants $K_{CMEO,DACA}$, determined at pH 5.22, 7.0, and 9.0, yielded values, respectively, of 8.2 ± 2.2, 9.7 ± 2.2, and 31.8 ± 1.7 μM. These measurements show that DACA has a higher affinity for the CME($NAD^+$) complex than for the E($NAD^+$) complex (with pH independent, $K_{EO,DACA}$ = 23 ± 6 μM; Dahl & Dunn, 1984).

(*F*) *Kinetics of CME(NAD⁺,DACA) Formation.* The time-resolved spectral changes which occur in the UV and visible regions upon mixing CME with $NAD^+$ and DACA are shown in Figure 3A. It is evident from the time dependence of the spectral changes that the 458-nm-absorbing CME($NAD^+$,DACA) species is formed as free DACA ($\lambda_{max}$ = 398

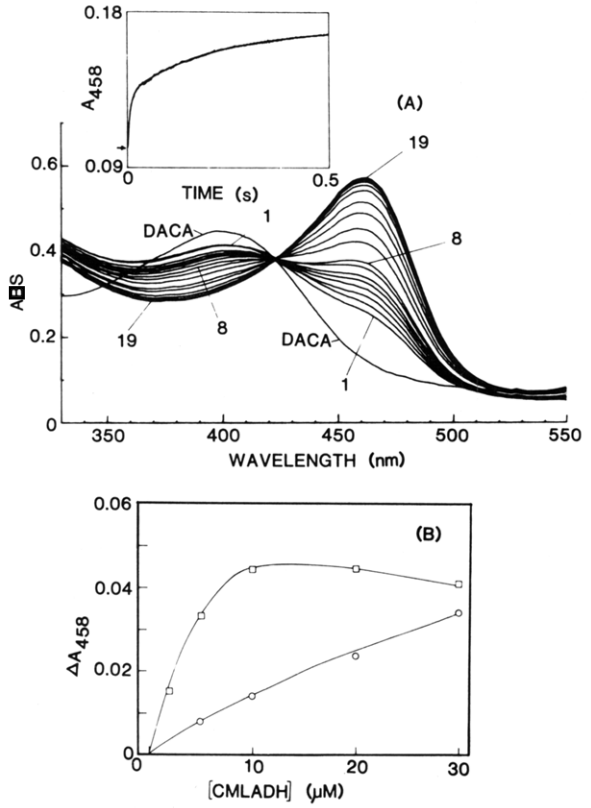


FIGURE 3: (A) Rapid-scanning stopped-flow spectra for the reaction of the CME(NAD$^+$) complex with DACA. Scanning was initiated 5.5 ms after flow had stopped. Scans 1–19 were collected with an 8.605-ms scan rate with initiation of each scan at the following times: (1) 5.5, (2) 14.1, (3) 31.3, (4) 39.9, (5) 48.5, (6) 57.1, (7) 74.3, (8) 91.6, (9) 126.0, (10) 177.6, (11) 263.6, (12) 349.7, (13) 521.8, (14) 693.9, (15) 926.2, (16) 1124.2, (17) 1554.4, (18) 2414.9, and (19) 4135.9 ms. Conditions were the following: for syringe A, 30 $\mu$N CMLADH and 10 $\mu$M DACA; for syringe B, 2 mM NAD$^+$. Both syringes contained 0.035 M TES/Na$^+$ buffer, pH 7.0. Scan 0 is the spectrum of free DACA obtained by mixing syringe A with buffer. All concentrations are those after mixing. Inset: Typical stopped-flow, rapid-mixing time course for the association of CMLADH with NAD$^+$ and DACA at 458 nm. Conditions were the following: for syringe A, 30 $\mu$N CMLADH; for syringe B, 5 $\mu$M DACA and 2 mM NAD$^+$. Both syringes contained 0.05 M TES/Na$^+$ buffer, pH 7.0. All concentrations are those after mixing. The observed trace is overlaid with the theoretical time course constructed from the computer best fit, assuming the reaction is a sum of two first-order reactions. The best-fit parameter for the fast phase was $k_{app}$ = 131 s$^{-1}$ (amplitude 0.028 A) and for the slow phase $k_{app}$ = 4.4 s$^{-1}$ (amplitude 0.039 A). (B) Dependence of the amplitudes for the fast and slow relaxations in the reaction of CMLADH with NAD$^+$ and DACA on the CMLADH concentration. The CMLADH concentration varied in syringe A, while for syringe B 5.0 $\mu$M DACA and 2 mM NAD$^+$ were present. Both syringes contained 0.05 M TES/Na$^+$ buffer, pH 7.0. The biphasic time courses were analyzed by nonlinear regression as the sum of two first-order reactions (A), and the resulting amplitudes of the fast (○) and slow (□) relaxations were plotted as a function of enzyme concentration.

nm) disappears. However, a considerable amount of CME(NAD$^+$,DACA) is also formed in the time required to record the first spectrum (5–10 ms), indicating that some CME(NAD$^+$,DACA) is formed in a fast (burst) phase. This fast phase is followed by slower formation of more CME(NAD$^+$, DACA).

The kinetics of this biphasic reaction were further investigated via single-wavelength stopped-flow measurements (inset to Figure 3A). The time course of the absorbance change at 458 nm confirms that the appearance of the CME(NAD$^+$, DACA) complex is biphasic. This is in contrast to the situation with native enzyme where, under similar conditions, formation

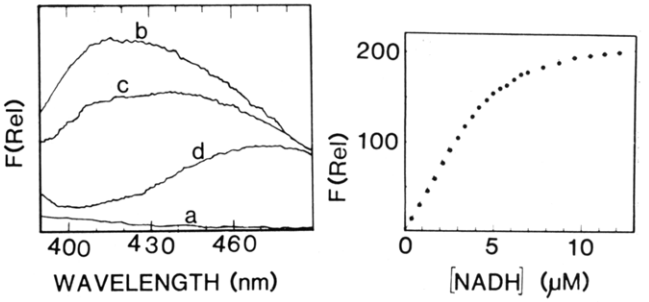


FIGURE 4: Fluorescence emission spectra (uncorrected) of NADH, CME(NADH), and CME(NADH,pyr). Excitation was at 330 nm. (a) Base line measured for 0.025 M TES/Na$^+$ buffer, pH 7.0; (d) after addition of 1.67 $\mu$M NADH; (c) after addition of 5.1 $\mu$N CMLADH; (b) after addition of 3.2 mM pyrazole. Inset: Fluorescence titration of CMLADH with NADH in the presence of excess pyrazole. Instrument settings: $\lambda_{ex}$ = 330 nm; $\lambda_{em}$ = 410 nm. Aliquots (10 $\mu$L) of NADH were titrated into a cuvette containing 6 $\mu$N CMLADH (concentration determined by using $A^1_{280nm}$ = 0.455), 5 mM ethanol, and 5 mM pyrazole in 25 mM TES/Na$^+$ buffer, pH 7.0. The fluorescence has been corrected for volume changes during the titration but not for the fluorescence of free NADH. Analysis via nonlinear regression gave a titration end point of 4.89 ± 0.08 $\mu$N, a dissociation constant, $K_{CMEpyr,R}$, of 0.25 ± 0.05 $\mu$M, and relative fluorescence coefficients for NADH and CME(NADH,pyr) of 2.7 ± 0.6 and 38.5 ● 0.8, respectively. The titration end point and the curve tangents shown on the figure are those computed.

of the E(NAD$^+$,DACA) complex is complete within the mixing dead time of the stopped-flow instrument (Dahl & Dunn, 1984).

To elucidate the nature of the biphasic time course, CME was mixed with NAD$^+$ and DACA at pH 7.0 in separate experiments where the concentrations of DACA and enzyme were varied. When 2.5 $\mu$N enzyme and 2.5–50 $\mu$M DACA concentrations are used, the total amplitude of the reaction is dominated by the amplitude of the slow phase; with 2.5 $\mu$M DACA, more than two-thirds of the total amplitude change occurs in the slow phase; at higher DACA concentrations, the fast phase could hardly be seen. The amplitude of the slow phase increases with increasing DACA concentration, reaching a saturated value at high DACA concentration. This is also evident from the binding experiments shown in Figure 2. However, the rate of the slow relaxation (3.4 ± 0.2 s$^{-1}$) is independent of DACA concentration.

Using a constant DACA concentration of 5.0 $\mu$M, we varied the CMLADH concentration from 2 to 30 $\mu$M. The biphasic time courses were analyzed as the sum of two first-order reactions. The results, summarized in Figure 3B, show that the amplitude of the slow phase first increases but then decreases with increasing enzyme concentration, while the amplitude of the fast phase only increased. The rate of the slow relaxation showed little dependence on CME concentration, while the rate of the fast relaxation increased from 53 s$^{-1}$ at 5.0 $\mu$N enzyme to 131 s$^{-1}$ at 30 $\mu$N enzyme.

The dissociation of DACA from the CME(NAD$^+$,DACA) complex was measured by preincubating CME (5 $\mu$N), NAD$^+$ (2 mM), an DACA (50 $\mu$M) in one syringe and rapidly mixing with pyrazole (20 mM) in 20 mM TES/Na$^+$ at pH 7.0. Upon mixing, the stable CME(NAD–pyr) adduct forms as DACA dissociates from the complex. In this experiment, DACA dissociation was observed as a very fast relaxation ($1/\tau \simeq 520$ s$^{-1}$).

*Properties of CME(NADH). (A) Binding of Pyrazole and 4-Methylpyrazole to CME(NADH).* The binding of the heterocycle imidazole is known to enhance the fluorescence of NADH bound to the native enzyme approximately 3-fold (Theorell & McKinley-McKee, 1961), while imidazole has

Scheme I

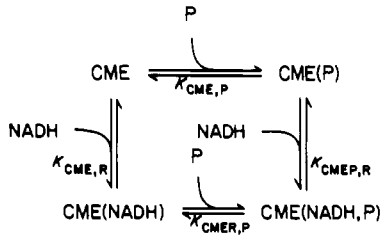


Table I: Summary of Dissociation Constants ($\mu$M) for Reaction of Pyrazole, 4-Methylpyrazole, and NADH with CMLADH according to Scheme II[a]

| | $K_{CME,R}$ | $K_{CMER,P}$ | $K_{CMEP,R}$ | $K_{CME,P}$ |
|---|---|---|---|---|
| pyrazole | 1.5 ± 0.5 | 197 ± 8 | 0.25 ± 0.05 | 1100 |
| 4-methylpyrazole | 1.5 ± 0.5 | 39 ± 2 | 0.30 ± 0.03 | 190 |

[a] The values are computed from fluorescence titration data. The titrations were done in duplicate or triplicate.

no such effect on the fluorescence of CME(NADH) (Reynolds & McKinley-McKee, 1975). In contrast to the behavior of imidazole, Figure 4 shows that pyrazole enhances the fluorescence of CME(NADH) at 410 nm by about 50%, indicating that a CME(NADH,pyr) complex is formed. A similar fluorescence enhancement was also observed with 4-methylpyrazole.

The stabilities of the binary, CME(NADH), and the ternary, CME(NADH,pyr) and CME(NADH,Me-pyr), complexes were measured in titrations where the enhancement of NADH fluorescence by CMLADH, pyrazole, and 4-methylpyrazole was utilized. Scheme I was assumed to describe the binding of NADH and P (pyrazole or 4-methylpyrazole) to CMLADH with the dissociation constants for the respective complexes as indicated.

$K_{CME,R}$ was determined from titration of CME with NADH, $K_{CMER,P}$ by titration of CME(NADH) with pyrazole or 4-methylpyrazole, and $K_{CMEP,R}$ by titration of CME(pyr) or CME(Me-pyr) with NADH. When titrating with or in the presence of NADH, we included ethanol (5 mM) to avoid oxidation of NADH by trace amounts of oxidizing material present as impurities (Reynolds & McKinley-McKee, 1975). When CME, CME(pyr), or CME(Me-pyr) was titrated with NADH, tight binding was observed, and the titration end point could also be computed. However, when CME(NADH) was titrated with pyrazole or 4-methylpyrazole, the complexes formed were weaker, and in order to achieve convergence in the regression analyses, the enzyme site concentrations were assigned values determined by other methods. Since pyrazole and 4-methylpyrazole have no fluorescence, the relative fluorescence coefficients for these species were kept fixed at zero. $K_{CME,P}$ was calculated by using the relationship

$$K_{CME,P} = \frac{K_{CME,R}K_{CMER,P}}{K_{CMEP,R}}$$

The inset to Figure 4, which shows the titration of the CME(pyr) complex with NADH, is typical of the fluorescence titration curves obtained.

The value obtained for $K_{CME,R}$ of 1.5 ± 0.5 $\mu$M (Table I) agrees with the value of 1.7 $\mu$M at pH 7.4 previously reported (Reynolds & McKinley-McKee, 1975) and with the kinetically determined value of 2.7 $\mu$M at pH 7.9 (Hardman, 1976). The calculate dissociation constants are summarized in Table I.

(*B*) *CME(NADH,DACA) Complex.* The reaction of the native E(NADH) complex with DACA takes place via the formation of a transient E(NADH,DACA) intermediate in

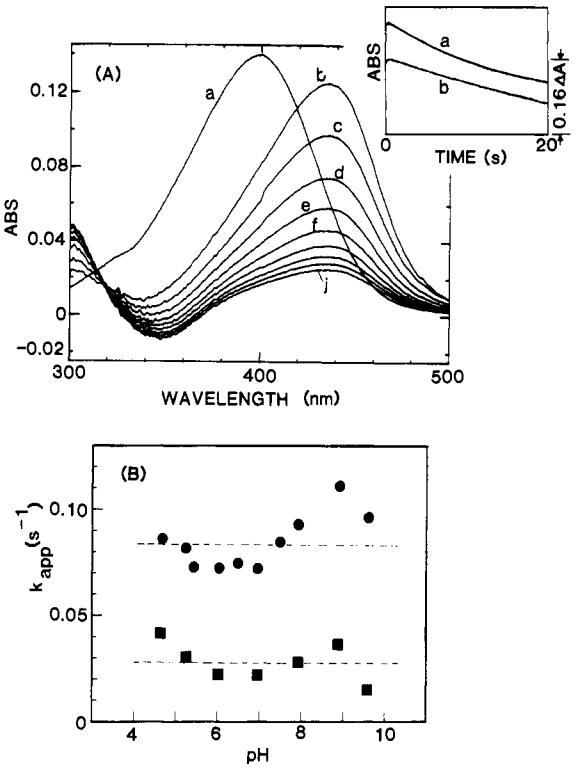


FIGURE 5: (A) Spectra of free DACA (a) and the decaying CME(NADH,DACA) complex (b–j). Spectrum a is that of 4.6 $\mu$M DACA in 0.1 M TES/$Na^+$ buffer, pH 7.0. Spectra of the CME(NADH, DACA) complex were obtained by balancing a cuvette containing 140 $\mu$N CMLADH and 140 $\mu$M NADH in 0.1 M TES/$Na^+$ buffer, pH 7.0 (total volume 0.75 mL). A small volume (5 $\mu$L) of concentrated DACA was then added to give a final concentration of 4.6 $\mu$M. The first spectrum (b) was recorded after 5 s, and the following spectra (c–j) were then recorded with 2.5-s intervals. Inset: Representative stopped-flow, rapid-mixing time courses for the decay of the CME(NADH,DACA) complex at pH 7.0 measured at 450 nm. Conditions were the following: (trace a) syringe A, 10 $\mu$N CMLADH and 3.0 $\mu$M NADH; syringe B, 50 $\mu$M DACA in 0.05 M TES/$Na^+$ buffer, pH 7.0; trace b same as trace a but with NADH replaced with NADD. Fitting of the decay curve to a single first-order reaction gave $k_{app}$ = 0.070 $s^{-1}$ for trace a and $k_{app}$ = 0.023 $s^{-1}$ for trace b. (B) Plot of the observed decay rate for the CME(NADH,DACA) (●) and CME(NADD,DACA) (■) complexes as a function of pH. Conditions were the following: syringe A, 10 $\mu$N CMLADH and 3 $\mu$M NADH (or NADD) in dilute TES/$Na^+$ buffer, pH 7.0; syringe B, 50 $\mu$M DACA in 0.05 M buffer. The final pH values were pH 4.64, 5.22, 5.43, 6.02, and 6.53 MES/$Na^+$ buffer; pH 6.94, 7.50, and 7.97 TES/$Na^+$ buffer; and pH 8.92 and 9.59 TAPS/$Na^+$ buffer. The pH values were measured on a mixture of equal volumes of the contents of syringes A and B. All concentrations are those after mixing. The rate values are those computed by fitting via nonlinear regression to a first-order decay reaction.

which the spectrum of DACA is red shifted from 398 to 464 nm. This intermediate becomes a quasi-stable species, E(NADH,DACA), at high pH (Dunn & Hutchison, 1973; Dunn et al., 1982). When DACA reacts with the CME(NADH) complex, a transient CME(NADH,DACA) intermediate also is formed, but in contrast to the situation with the native enzyme, the intermediate is not stabilized by high pH. Figure 5A shows that the absorption spectrum of DACA ($\lambda_{max}$ = 398 nm, $\epsilon_{398}$ = 3.10 × $10^4$ $M^{-1}$ $cm^{-1}$; Dunn & Hutchison, 1973) is red shifted to 436 nm as the CME(NADH, DACA) intermediate is formed. As seen from the decrease of the 436-nm band, the intermediate then undergoes a time-dependent decay. By extrapolation of the absorption of the 436-nm band to time zero, the extinction coefficient is estimated to be $\epsilon_{436}$ = 3.9 × $10^4$ $M^{-1}$ $cm^{-1}$. Figure 5A also shows that the decay of the 436-nm band is concomitant with a decrease in the 340-nm region, indicating that decay of the

intermediate is coupled to NADH oxidation and aldehyde reduction.

Various LADH inhibitors were tested as potential "suicide" reagents for restricting the CME-catalyzed reduction of DACA to a single turnover. However, a suitable inhibitor was not found; consequently, limitation of the reaction to a single turnover was accomplished instead by using limiting amounts of NADH. Trace a in the inset to Figure 5A shows a typical decay curve for the reduction of DACA where the concentrations of both CMLADH and DACA are in excess of the NADH concentration. Since [NADH] is limiting, the decay reaction represents only a single turnover of enzyme-bound coenzyme. Under these conditions, the formation of the CME(NADH,DACA) intermediate is too fast to be measured by the stopped-flow technique. Computer fitting of the reaction trace (viz., the inset to Figure 5A) by nonlinear regression demonstrates that the reaction is well described by the rate law for a first-order decay process.

The stopped-flow technique was used also to determine how the decay of the CME(NADH,DACA) intermediate during substrate reduction depends on pH. From these results which are summarized in Figure 5B, it is clear that the decay rate shows only a minor dependence on pH in the region from pH 4.6 to pH 9.6. The differences observed could as well be due to the different buffer ions used. The observed pH dependence is in marked contrast to what was observed for the native enzyme where the decay of the E(NADH,DACA) intermediate depends on protonation of a group with apparent $pK_a$ = 6.0 (Morris et al., 1980). In order to verify this contrasting pH dependence between the native and the carboxymethylated enzymes, we also measured the decay of the native E(NADH,DACA) intermediate using limiting NADH. It was observed that the decay rates measured by using this method are identical (within the limit of experimental error) with the rates measured earlier (Morris et al., 1980).

When NADD is substituted for NADH, the decay of the intermediate is slowed. Traces a and b in the inset to Figure 5A compare typical decay time courses for NADH and NADD. It is evident from this comparison that the reaction is subject to a primary, kinetic, isotope effect with $k_H/k_D$ = 3.0. The observed isotope effect shows that hydride transfer is involved in the step which is rate limiting for the decay of the intermediate.

The rate of CME(NADD,DACA) decay was also studied as a function of pH. Figure 5B shows that deuterium substitution does not alter the pH dependence and that the isotope effect is constant with $k_H/k_D$ = 3.0 over the pH range studied. This is also in contrast to what was observed for the native enzyme where a primary isotope effect with $k_H/k_D$ = 3.0 was observed at low pH, while this ratio decreased to 1.0 (i.e., no isotope effect) at higher pH (Morris et al., 1980).

Due to the decay of the CME(NADH,DACA) intermediate at all pH values investigated, the rapid-mixing stopped-flow technique was used to follow the appearance of the intermediate. By varying the concentration of DACA and by working on time scales where the decay of the intermediate is negligible (i.e., 100 ms), we determined the binding isotherm from the amplitude of the absorbance change at 450 nm. Using nonlinear regression to analyze the resulting binding isotherm (data not shown), we computed the apparent dissociation constant $K_{CMER,DACA}$(app) to be 18 ± 4 μM at pH 7.0. In a similar way, $K_{CMR,DACA}$(app) was computed to be 16 ± 3 μM at pH 5.2 (0.05 M MES/$Na^+$ buffer) and 35 ± 5 μM at pH 9.0 (0.05 M TAPS/$Na^+$ buffer). Since $K_{ER,DACA}$ was found to be 4 μM by using a similar method or 7 μM when calculated

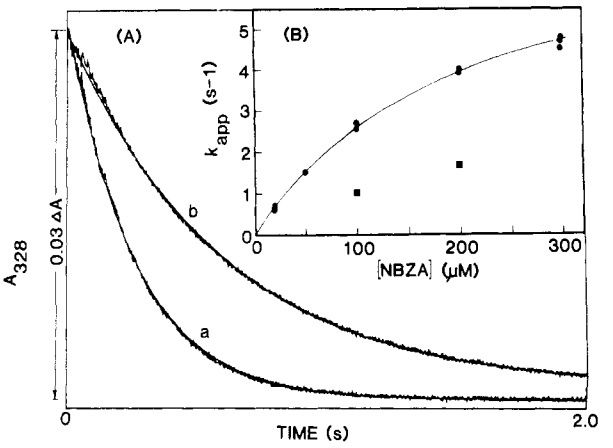


FIGURE 6: (A) Representative stopped-flow, rapid-mixing time courses comparing the effects of substituting NADH with NADD for the CMLADH-catalyzed transient reduction of NBZA at pH 7.0. Conditions were the following: (trace a) syringe A, 20 μN CMLADH and 10 μM NADH; syringe B, 200 μM NBZA. Both syringes contained 0.05 M TES/$Na^+$ buffer, pH 7.0. Trace b, same conditions as trace a but with NADH replaced with NADD. All concentrations are those after mixing. Computer fitting to a single first-order reaction gave $k_{app}$ = 3.9 $s^{-1}$ (amplitude 0.031 A) for trace a and $k_{app}$ = 1.7 $s^{-1}$ (amplitude 0.029 A) for trace b. The experimental traces are overlaid with the computer-generated best-fit curves. (B) Apparent first-order rate constant for the reaction of CME(NADH) (●) or CME(NADD) (■) with NBZA as a function of NBZA concentration. Conditions were 20 μN CMLADH and 10 μM NADH (or NADD) in 0.05 M TES/$Na^+$ buffer, pH 7.0. The rate constants are from single-wavelength time courses like those in (A). Analysis via nonlinear regression gave $K_D$ = 190 ± 10 μM and $k_{max}$(app) = 7.7 ± 0.3 $s^{-1}$. The curve shown is the computer best fit.

from kinetic measurements (Dunn & Hutchinson, 1973), carboxymethylation labilizes the E(NADH,DACA) complex.

Comparison of the steady-state turnover rates for DACA reduction catalyzed by native and carboxymethylated enzyme showed that at pH 7.0, CMLADH has about 15% of the activity of the native enzyme, while at pH 9.5 CMLADH is 3-fold more active. That carboxymethylation gives an enzyme which is more active in catalyzing the aldehyde reduction at high pH is in agreement with the earlier findings of Reynolds & McKinley-McKee (1975).

*Transient Kinetics for the CMLADH-Catalyzed Reduction of NBZA.* The CME-catalyzed reduction of NBZA by NADH and NADD was studied by the rapid-mixing stopped-flow technique by following the disappearance of NADH at 328 nm. As with the reduction of DACA, limiting amounts of NADH were used to restrict the reaction to one turnover. Figure 6A shows that the reduction follows a first-order time course. When NADH is substituted with NADD, a primary kinetic isotope effect with $k_H/k_D$ = 2.3 is observed, indicating that hydride transfer is a component of the rate-limiting step for the reaction. The saturation curve shown in Figure 6B corresponds to an apparent dissociation constant $K_D$ = 190 ± 10 μM and a $k_{max}$(app) = 7.7 ± 0.3 $s^{-1}$.

## Discussion

The carboxymethylation of LADH is a well-defined and specific reaction where almost exclusively Cys-46 is the site of modification (Harris, 1964; Reynolds & McKinley-McKee, 1969; Dahl & McKinley-McKee, 1981a). Although the catalytic activity is greatly reduced, the modified enzyme is still a highly effective catalyst. The X-ray structure of CMLADH shows that the thioether sulfur of carboxymethylated Cys-46 is still ligated to the active-site metal ion and the carboxyl group appears to be oriented toward the general anion binding site and Arg-369 (Zeppezauer et al., 1975). The

Table II: Summary of the Spectral Properties of DACA and the Dissociation Constants for the Different Ternary Complexes Formed with DACA

| compd | $\gamma_{max}$ (nm) | $\epsilon$ ($\times 10^{-4}$ $M^{-1}$ $cm^{-1}$) | red shift ($\Delta$nm) | dissociation constant[c] | value ($\mu$M) |
|---|---|---|---|---|---|
| DACA[a] | 398 | 3.10 | | | |
| E(NADH,DACA)[a] | 464 | 6.20 | 66 | $K_{ER,DACA}$ | 4 (or 7) |
| E($NAD^+$,DACA)[b] | 495 | 6.0 | 97 | $K_{EO,DACA}$ | 23 ± 6 |
| CME(NADH,DACA) | 436 | 3.9 | 38 | $K_{CMER,DACA}$ | 18 ± 4 |
| CME($NAD^+$,DACA) | 458 | 7.2 | 60 | $K_{CMEO,DACA}$ | 9.7 ± 2.2 |

[a] Dunn & Hutchison (1973). [b] Dahl & Dunn (1984). [c] Constants for the dissociation of DACA from the indicated ternary complexes.

carboxymethylation of LADH can then be predicted to produce two important changes in the enzyme active site.

(1) The introduction of the carboxylate group changes the electrostatic forces in the active site. This negatively charged group is likely to be (partially) neutralized by forming a salt bridge with one of the arginine residues (47 or 369) at the general anion binding site. Note that a salt bridge between Arg-369 and Glu-68 is present in the X-ray structures of free LADH (Eklund et al., 1976) and of the E(NADH,dimethyl sulfoxide) complex (Eklund et al., 1981). In addition to electrostatic effects, the carboxymethyl group must produce some steric hindrance in the active site.

(2) The alkylation of Cys-46 replaces the negatively charged cysteinyl thiolate ion with the neutral thioether of the *S*-(carboxymethyl)cysteinyl residue which still ligates the active-site metal. The other two protein ligands to this metal are the neutral imidazole ring of His-67 and the thiolate ($RS^-$) of Cys-174 (Brändén et al., 1975). This change in the inner coordination sphere implies that the net formal charge of the active-site $Zn^{2+}$ is increased from approximately 0 to 1+ upon carboxymethylation. If other effects are ignored, these changes should increase the acidity of ionizable ligands (i.e., $H_2O$ or alcohol) in the fourth coordination position.

*Complexes Formed with DACA. (A) CME($NAD^+$,DACA) Complex.* Formation of the CME($NAD^+$,DACA) complex (Figures 2 and 3) red shifts the absorption of DACA 60 nm, while a 97-nm red shift is seen upon formation of E($NAD^+$,DACA) (Table II). The effect of carboxymethylation on E($NAD^+$,DACA) is thus a 37-nm blue shift.

Two factors are primarily responsible for the red-shifted spectrum of the E($NAD^+$,DACA) complex. First the carbonyl of DACA is coordinated to and polarized by the active-site metal (Scheme II). These interactions stabilize the excited form in the $\pi,\pi^*$ transition, making the excitation energy smaller and thereby shifting the absorption band to longer wavelength (Scheme II). Second, the close proximity of the carbonyl of DACA to the positively charged nicotinamide ring of $NAD^+$ introduces an additional electrostatic interaction. This positive charge will also stabilize the excited form and is considered to be the reason for the 31-nm greater red shift on formation of E($NAD^+$,DACA) compared to E(NADH,DACA) (Dahl & Dunn, 1974).

*(B) CME(NADH,DACA) Intermediate.* Upon reaction with the CME(NADH) complex, the absorption maximum of DACA is red shifted 38 nm from 398 to 436 nm (Figure 5). This red shift is 28 nm smaller than the corresponding red shift observed upon formation of the E(NADH,DACA) intermediate (Dunn & Hutchison, 1973); hence, the effect of carboxymethylation on the spectrum of the intermediate is a 28-nm blue shift. The red-shifted spectrum of the E(NADH,DACA) complex must also be due to coordination of the aldehyde carbonyl oxygen to the active-site metal. Using the same arguments as for the E($NAD^+$,DACA) complex above, we conclude that the blue shift observed upon carboxymethylation of the E(NADH,DACA) complex must be due to an opposing electrostatic interaction between the introduced carboxylate group and the negatively charged oxygen of the excited form of DACA.

Scheme II

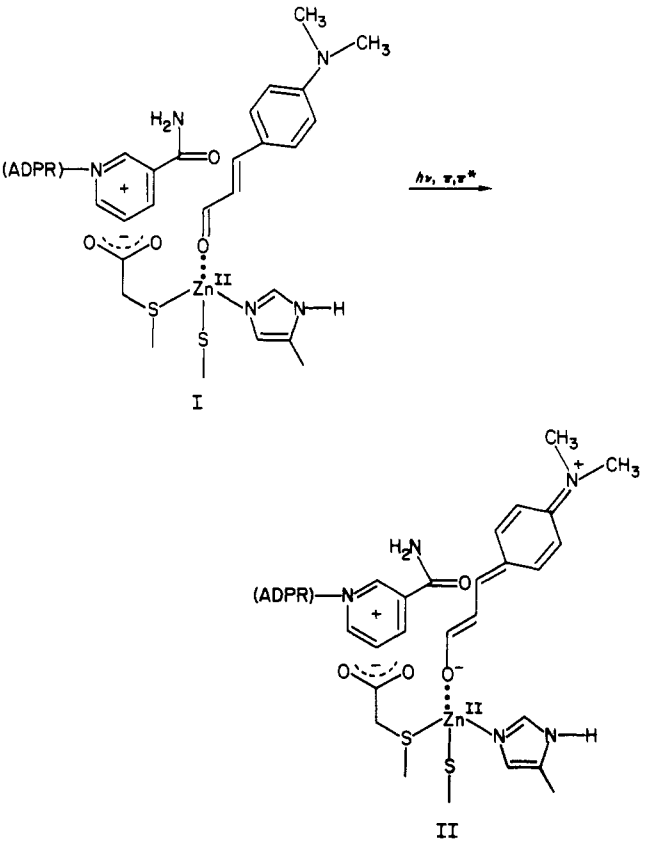


The spectral properties of the four different enzyme–coenzyme–DACA complexes characterized here and in previous work are summarized in Table II. The variation in observed red shifts illustrates that the DACA chromophore is a sensitive probe of the microenvironment within the active site. The magnitude of the red shift of the E(NADH,DACA) intermediate has been shown to depend upon the Lewis acid strength of the metal ion substituted for zinc in the active site of LADH (Dunn et al., 1982). When $Zn^{2+}$ is substituted with other metals, the following $\lambda_{max}$ values are observed: 478 nm ($Co^{2+}$), 475 nm ($Ni^{2+}$), and 457 nm ($Cd^{2+}$), indicating that increased Lewis acidity (with the expected order $Co^{2+} > Ni^{2+} \simeq Zn^{2+} > Cd^{2+}$) gives larger red shifts. This work and our previous study (Dahl & Dunn, 1984) demonstrate that DACA is sensitive both to the electrophilicity of the catalytic metal ion and to the electrostatic force fields contributed by proximate groups.

*(C) CME($NAD^+$,DMOX) Complex.* Figure 1 shows that, like native LADH, CMLADH forms a ternary complex with $NAD^+$ and (*Z*)-DMOX. The spectrum of (*Z*)-DMOX within the CME($NAD^+$,DMOX) complex is red shifted 80 nm. This red shift is quite similar to the 76-nm red shift which characterizes the formation of the E($NAD^+$,DMOX) complex (Abdallah et al., 1984). These observations show that the

spectrum of DMOX is far less sensitive to carboxymethylation than is the spectrum of DACA. That DMOX and DACA have different properties with respect to sensitivity to electrostatic effects in the enzyme active site must be due to different binding modes in the ternary complexes. It has been proposed that (*Z*)-DMOX forms a covalent adduct through bonding of either the nitrogen or the oxygen atom of the oxime to the 4-position of the nicotinamide ring of $NAD^+$, while either the oxygen or the nitrogen is ligated to the active-site metal, viz., structures III and IV (Abdallah et al., 1984). That

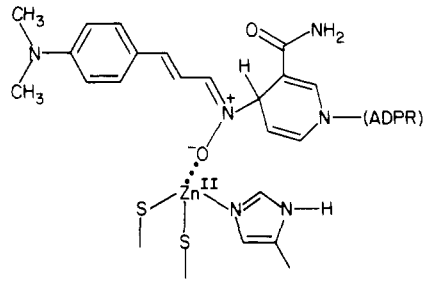

III

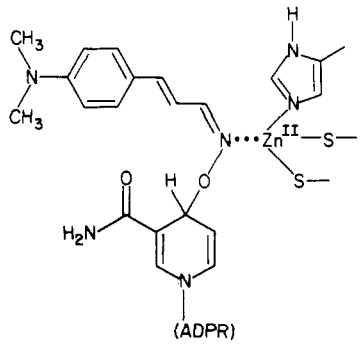

IV

carboxymethylation has little effect on the E[$NAD^+$,(*Z*)-DMOX] complex should be seen in connection with the observation of Abdallah et al. (1984) that the enzyme lacking zinc ion at the active sites is still capable of forming a complex with $NAD^+$ and (*Z*)-DMOX with spectral properties very similar to those of the native enzyme complex. That the spectral properties of the E[$NAD^+$,(*Z*)-DMOX] complex are rather inert both to carboxymethylation and to removal of the active-site metal shows that (*Z*)-DMOX binds to the active site in a different mode than does DACA, probably by forming an adduct with $NAD^+$ via the oxime nitrogen.

*(D) CME(NADH,pyr) and CME(NADH,Me-pyr) Complexes.* Binding of both pyrazole and 4-methylpyrazole to CME(NADH) enhances the fluorescence of NADH (Figure 4). By utilizing this fluorescence increase, we have determined the dissociation constants for the components of these complexes (Table I). Both pyrazole and 4-methylpyrazole have markedly higher affinities for CME(NADH) than for E(NADH) ($K_{CMER,pyr}$ = 197 ± 8 μM, while $K_{ER,pyr}$ previously has been determined to be 4 ± 1 mM; Andersson et al., 1981). Thus, carboxymethylation of LADH increases the affinity of the enzyme–NADH complex for pyrazole some 20-fold. Similarly, carboxymethylation also increases the free enzyme affinity for pyrazole [$K_{CME,pyr}$ = 1.1 mM (Table I) while $K_{E,pyr}$ = 8 mM (Andersson et al., 1981)]. The difference in affinity between LADH and CMLADH is likely due to the greater Lewis acidity of the active-site metal in CMLADH.

The same trend is seen in the tighter binding of both pyrazole and 4-methylpyrazole to the native E($NAD^+$) complex. It is also evident from the data in Table I that both pyrazole and 4-methylpyrazole have synergistic effects on the binding of NADH to CMLADH and visa versa.

That a rather stable CME(NADH,pyr) complex is formed is obviously the reason why the pyrazole suicide method used with the native enzyme (McFarland & Bernhard, 1972) fails to bring about a single turnover in the CME-catalyzed reduction of aldehydes.

*Kinetics. (A) Kinetics of CME($NAD^+$,DACA) Formation.* In the present work, it has been shown that formation of the CME($NAD^+$,DACA) and E($NAD^+$,DACA) complexes occurs via different mechanisms. The experimental results presented in Figures 2 and 3 led us to propose the following mechanism for formation and decay of the CME($NAD^+$,-DACA) complex:

$$\text{CME}(NAD^+) \overset{\tau_2}{\rightleftharpoons} \text{CME}(NAD^+)^* \quad (1)$$

$$\text{CME}(NAD^+)^* + \text{DACA} \overset{\tau_1}{\rightleftharpoons} \text{CME}(NAD^+,\text{DACA})^* \quad (2)$$

In this mechanism, the fast phase ($\tau_1$) of the time course involves the binding of DACA to the reactive CME($NAD^+$)* complex. The reacting system also involves a slow step ($\tau_2$) in which some chemical or conformational change limits the rate of interconversion of inactive and reactive forms of the CME($NAD^+$) complex. This slow interconversion accounts for the observed slow phase in the formation of the CME($NAD^+$,DACA) complex, a process that is independent of the concentration of both DACA and CMLADH. Since at equilibrium CME($NAD^+$) predominates when [DACA] > [CME], the amplitude of the slow phase is dominant. At equilibrium, the distribution of [CME($NAD^+$)]/[CME($NAD^+$)*] is estimated to be about 4 to 1. Consequently, as the ratio [CME]/[DACA] is increased, a greater fraction of DACA reacts directly with preexisting CME($NAD^+$)*, and the relative amplitude of the fast phase increases and then becomes dominant.

In the experiment where pyrazole is mixed with the CME($NAD^+$,DACA)* complex, pyrazole seems to react directly with the CME($NAD^+$)* complex at a rate which is limited by the dissociation of DACA. The observed fast relaxation is then a direct measure of the rate constant for DACA dissociation.

*(B) Transient Kinetics of DACA Reduction.* Figure 5 shows that under single-turnover conditions the decay of the CME(NADH,DACA) intermediate is essentially independent of pH from pH 5 to pH 9. A primary kinetic isotope effect of 3 for the decay reaction is observed over the whole pH interval, indicating that hydride transfer is a component of the rate-limiting step for intermediate decay. These observations show that the DACA reducing properties of CMLADH are quite different from those of the native enzyme.

The rate of hydride transfer is 80-fold slower with CME (0.084 vs. 7.2 $s^{-1}$), and pH effects on the decay of the DACA intermediate are quite different; decay of CME(NADH,-DACA) is pH independent, while decay of E(NADH,DACA) is driven by protonation of a group with apparent $pK_a$ = 6.0 (Morris et al., 1980).

The most interesting difference between native and carboxymethylated LADH is the pH dependence of intermediate decay. The pH independence found for CME explains the steady-state behavior of CMLADH. Steady-state rate measurements show that at high pH CME is more active than native LADH in the reduction of DACA and other aldehydes. Even though the hydride transfer step in CMLADH is much slower than in LADH, the process which becomes rate limiting for LADH at high pH is not rate limiting for CMLADH; thus, the CME turnover rate becomes faster at high pH. Morris

Scheme III

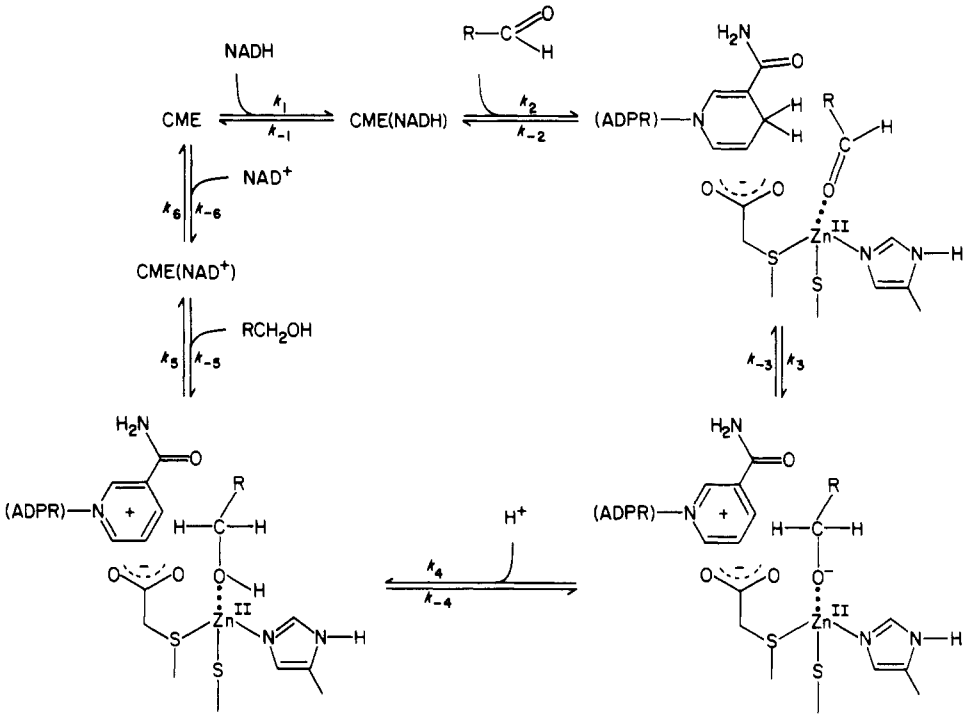


et al. (1980) reported that at pH 9.0, the E(NADH,DACA) decay rate is 0.011 $s^{-1}$, a value which is considerably slower than the CME(NADH,DACA) decay rate observed in the present work.

What are the mechanistic reasons for the slow hydride transfer rate and the lack of pH dependence in DACA reduction with the CME? Since we have no reason to anticipate that CMLADH catalyzes aldehyde reduction by a different mechanism (i.e., no other intermediates are involved), then the difference between LADH and CMLADH must result from the alteration of kinetic parameters in the overall mechanism, viz., Scheme III. Scheme III is adapted from the mechanism proposed by Morris et al. (1980) for the reduction of DACA. As shown in this scheme, the close proximity of the carboxymethyl group could affect hydride transfer by influencing (1) the activation of NADH for hydride donation, (2) the activation of the aldehyde for hydride acceptance, and/or (3) the positioning of the aldehyde and the nicotinamide ring relative to each other. It would be speculative to try to point out which way is the most important.

Several groups in the active site of the native enzyme might be responsible for the pH dependence of the decay process, but it seems reasonable that the alcohol/alcoholate exchange (step $k_4$, $k_{-4}$ in Scheme III) is of major importance (Morris et al., 1980; Dunn et al., 1982). According to Scheme III, proton uptake by the alcoholate complex to form alcohol is an obligatory step which occurs subsequent to hydride transfer (step $k_3$, $k_{-3}$) but which precedes alcohol release (step $k_5$, $k_{-5}$) in the aldehyde reduction. If we assign the pH-dependent decay of the E(NADH,DACA) intermediate (with apparent $pK_a$ = 6.0) to this proton transfer event,[2] then the difference between LADH and CMLADH is clearly explained by a shift in the apparent $pK_a$ of the coordinated alcohol which is induced by the carboxymethyl group. The $pK_a$ of an alcohol substrate is drastically decreased from about 16 ($pK$ = 15.9 for ethanol; Ballinger & Long, 1960) to an *apparent value* of about 6 in the ternary E($NAD^+$,alc) complex. If carboxymethylation perturbs this shift so that there is a smaller decrease in the apparent $pK_a$ of the ternary CME($NAD^+$,alc) complex[2] (i.e., to a value >9), then the kinetics of intermediate decay would be essentially independent of pH below 9.

That carboxymethylation can induce such a shift in the $pK_a$ of alcohol/alcoholate not only is possible but also is highly reasonable. In the free enzyme, an apparent $pK_a$ = 9.2 controls coenzyme binding. There is a group with apparent $pK_a$ = 11.2 in the E(NADH) complex which controls DACA binding, and there is a group with apparent $pK_a$ = 7.4 in the E($NAD^+$) complex which controls alcohol binding (Andersson et al., 1980a,b, 1981). It has been proposed by various workers that a single ionizable group, the zinc-coordinated water molecule, is responsible for these pH dependencies and that the different apparent $pK_a$ values arise from perturbation of the $pK_a$ of this moiety.

Since upon formation of the ternary complex alcohol is presumed to replace the coordinated water molecule, interactions with the positively charged nicotinamide ring of $NAD^+$ and the CME-carboxylate undoubtedly influence the alcohol/alcoholate $pK_a$. Consequently, the apparent $pK_a$ of the coordinated DACA–alcohol[2] could shift from 6.0 to a value >9 (Figure 5B) on going from E($NAD^+$,alc) to CME-($NAD^+$,alc).

The observed lack of inhibition by TFE can also be explained by a $pK$ shift in the metal-bound alcohol/alcoholate. TFE forms a stable E($NAD^+$,TFE) complex and hence is a potent inhibitor of LADH. The $pK_a$ of TFE is shifted from 12.4 (Ballinger & Long, 1960) to an apparent value of 4.3 within the ternary complex (Kvassmann & Pettersson, 1980a). Therefore, at neutral pH, TFE is tightly bound (presumably as the alkoxide ion), and thus the inhibitory effect. However, if in the CME($NAD^+$,TFE) complex the apparent $pK$ of TFE is shifted to a higher value (≥7), then TFE would bind con-

[2] According to Scheme III, the pH-dependent rate of decay of the E(NADH,DACA) intermediate is described by the expression

$$k_{obsd} = \frac{k_3[\text{E(NADH,DACA)}][H^+]}{K_a(k_{-3}/k_5) + [H^+]}$$

where $K_a = k_{-4}/k_4$, the microscopic constant for ionization of a proton from the coordinated DACA–alcohol–enzyme–$NAD^+$ complex (Morris et al., 1980; Dunn et al., 1982), and therefore the *apparent* $pK_a$ is given by $pK_{app} = -\log [K_a(k_{-3}/k_5)]$.

siderably more weakly and hence the lack of an appreciable inhibitory effect. This prediction agrees with the observation that the $pK_a$ for the quenching of the intrinsic enzyme fluorescence in the E($NAD^+$,TFE) complex is shifted from $\leq 4.0$ to $\leq 6.4$ upon carboxymethylation (Parker et al., 1978).

When Hardman (1976) studied alcohol oxidation with CMLADH, he found that the rate-limiting process for turnover (which he concluded to be hydride transfer) is 700-fold slower than with the native enzyme. In the present work, we have shown that the rate of hydride transfer in the direction of aldehyde reduction is 80-fold slower than with the native enzyme. We think this difference can be explained by the effect of the introduced carboxylate group on the $pK_a$ of the alcohol in the complex with $NAD^+$. In alcohol oxidation, the conversion of coordinated alcohol to alcoholate (step $k_4$, $k_{-4}$, Scheme III) appears to be a fast preequilibrium step (involving proton release) which precedes hydride transfer. When this equilibrium is shifted in the direction of bound alcohol (via perturbation of the $pK_a$), the observed rate of oxidation (formation of NADH) will be attenuated by the unfavorable shift in the equilibrium concentration of coordinated alkoxide ion. However, the appearance of NADH will still be subject to a primary isotope effect when alcohol deuterated at the C-1 position is substituted for isotopically normal substrate. In conclusion, we think that the 700-fold slower alcohol oxidation with CMLADH is partially due to a shift in the alcohol/alcoholate equilibrium within the ternary complex.[3]

*(C) Transient Reduction of NBZA.* Due to the electron-withdrawing effect of the *p*-nitro group, the aldehyde carbon of NBZA is electron deficient and hence a very potent hydride acceptor, and consequently, NBZA is a good substrate for LADH. Under single-turnover conditions, the reaction of NBZA with E(NAD) is a biphasic reaction. The fast phase ($k_{obsd} > 400\ s^{-1}$; Dunn et al., 1979; Andersson & Pettersson, 1982) is subject to a primary isotope effect ($k_H/k_D \simeq 2.0$) when NADH is substituted with NADD. The slow phase ($k_{obsd} = 0.5\ s^{-1}$ at pH 8.75) is nearly independent of substrate concentration and shows no isotope effect (Dunn et al., 1979; Koerber & Dunn, 1981). The transient kinetic behavior of NBZA is quite different when reduction is catalyzed by CME. Under single-turnover conditions, only a single phase is observed (Figure 6A). The rate of this apparent first-order process is subject to a primary isotope effect of $k_H/k_D = 2.3$ when NADD is substituted for NADH. When extrapolated to infinite substrate concentration, the rate data (Figure 6B) predict a $k_{max}(app) = 7.7 \pm 0.3\ s^{-1}$. The rate constant for hydride transfer in the reduction of NBZA at saturating substrate concentration has previously only been measured with cobalt-substituted LADH ($k_{obsd} = 150\ s^{-1}$). At high substrate concentrations, reaction with the zinc enzyme becomes too fast to be measured with stopped-flow methods (Koerber et al., 1983). Assuming that carboxymethylation retards the hydride transfer 80-fold (as was found for DACA) gives a value of approximately $620\ s^{-1}$ for the native enzyme, in reasonable agreement with values estimated previously (Dunn et al., 1979; Andersson & Pettersson, 1982).

In conclusion, carboxymethylation of Cys-46 brings about a highly selective chemical modification of LADH which significantly alters the energies of gound states and transition states along the catalytic path. Nevertheless, in comparison to nonenzymatic model systems, CMLADH still is a highly efficient catalyst. The altered catalytic properties of CMLADH almost certainly originate from the electrostatic effects brought about by the introduction of the negatively charged CM-carboxylate moiety into the catalytic site. The close proximity of this negative charge to the reacting atoms (i.e., the active-site zinc, the substrate functional group, and the 4-position of the nicotinamide ring) alters the electrostatic field experienced by these atoms during catalysis, making hydride transfer a less favorable process. This negative charge opposes both the Lewis acid role played by zinc ion in the activation of the aldehyde carbonyl for hydride attack and the ionization of inner-sphere-coordinated alcohol, thereby decreasing the concentration of coordinated alkoxide, the reactive species in alcohol oxidation.

Very clearly, the investigation of enzyme derivatives such as CMLADH which retain catalytic activity, albeit modified, has the potential of contributing a more richly detailed description of the conformational changes, the bonding forces, and the electrostatic interactions which convey catalytic activity to LADH.

[3] A shift of approximately 1 $pK_a$ unit to higher pH together with a decrease in the hydride transfer rate constant by a factor of 80 would explain the 700-fold lower rate observed by Hardman (1976). Unpublished work (M. J. Hardman, private communication) indicates carboxymethylation brings about a $pK_a$ perturbation of this magnitude.

Acknowledgments

We thank Dr. Michael Hardman for discussions concerning the interpretation of the $pK_a$ perturbations which we propose to explain the effects of carboxymethylation on alcohol oxidation and for providing us with unpublished data for the pH dependence of alcohol oxidation.

References

Abdallah, M. A., Biellmann, J.-F., Cedergren-Zeppezauer, E., Gerber, M., Dietrich, H., Zeppezauer, M., Koerber, S. C., MacGibbon, A. K. H., & Dunn, M. F. (1984) *Biochemistry 23*, 1003–1015.

Andersson, P., & Pettersson, G. (1982) *Eur. J. Biochem. 122*, 559–568.

Andersson, P., Kvassmann, J., Lindström, A., Oldén, B., & Pettersson, G. (1980a) *Eur. J. Biochem. 108*, 303–312.

Andersson, P., Kvassmann, J., Lindström, A., Oldén, B., & Pettersson, G. (1980b) *Eur. J. Biochem. 113*, 425–433.

Andersson, P., Krassman, J., Lindström, A., Oldén, B., & Pettersson, G. (1981) *Eur. J. Biochem. 114*, 549–554.

Angelis, C. T., Dunn, M. F., Muchmore, D. C., & Wing, R. M. (1977) *Biochemistry 16*, 2922–2931.

Ballinger, P., & Long, F. A. (1960) *J. Am. Chem. Soc. 82*, 795–798.

Brändén, C.-I., Jörnvall, H., Eklund, H., & Furugren, B. (1975) *Enzymes, 3rd Ed. 11*, 103–190.

Dahl, K. H., & McKinley-McKee, J. S. (1981a) *Eur. J. Biochem. 118*, 507–513.

Dahl, K. H., & McKinley-McKee, J. S. (1981b) *Eur. J. Biochem. 120*, 451–459.

Dahl, K. H., & Dunn, M. F. (1984) *Biochemistry 23*, 4094–4100.

Dalziel, K. (1957) *Acta Chem. Scand. 11*, 397–398.

Dietrich, H., Maret, W., Wallén, L., & Zeppezauer, M. (1979) *Eur. J. Biochem. 100*, 267–270.

Dietrich, H., MacGibbon, A. K. H., Dunn, M. F., & Zeppezauer, M. (1983) *Biochemistry 22*, 3432–3438.

Dunn, M. F., & Hutchison, J. S. (1973) *Biochemistry 12*, 4882–4892.

Dunn, M. F., Biellmann, J.-F., & Branlant, G. (1975) *Biochemistry 14*, 3176.

Dunn, M. F., Bernhard, S. A., Anderson, D., Copeland, A., Morris, R. G., & Rogue, J.-P. (1979) *Biochemistry 18*, 2346–2354.

Dunn, M. F., Dietrich, H., MacGibbon, A. K. H., Koerber, S. C., & Zeppezauer, M. (1982) *Biochemistry 21*, 354–363.
Eklund, H., Nordström, B., Zeppezauer, E. Söderlund, G., Ohlsson, I., Boiwe, T., Söderberg, B.-O., Tapia, O., Brändén, C.-I., & Åkeson, Å. (1976) *J. Mol. Biol. 102*, 27–59.
Eklund, H., Samama, J.-P., Wallén, L., Brändén, C.-I., Åkesson, Å., & Jones, T. A. (1981) *J. Mol. Biol. 146*, 561–587.
Evans, N., & Rabin, B. R. (1968) *Eur. J. Biochem. 4*, 548–554.
Hardman, M. J. (1976) *Eur. J. Biochem. 66*, 401–404.
Harris, I. (1964) *Nature (London) 203*, 30–34.
Hennecke, M., & Plapp, B. V. (1983) *Biochemistry 22*, 3721–3728.
Jones, D. T., & Khalifah, R. G. (1980) *Adv. Exp. Med. Biol. 132*, 77–83.
Khalifah, R. G., & Sutherland, W. M. (1979) *Biochemistry 18*, 391–398.
Koerber, S. C., & Dunn, M. F. (1981) *Biochimie 63*, 97–102.
Koerber, S. C., MacGibbon, A. K. H., Dietrich, H., Zeppezauer, M., & Dunn, M. F. (1983) *Biochemistry 22*, 3424–3431.
Kvassmann, J., & Pettersson, G. (1980a) *Eur. J. Biochem. 103*, 557–564.
Kvassmann, J., & Pettersson, G. (1980b) *Eur. J. Biochem. 103*, 565–575.
Li, T.-K., & Vallee, B. L. (1964) *Biochemistry 3*, 869–873.
McFarland, J. T., & Bernhard, S. A. (1972) *Biochemistry 11*, 1486–1493.
Morris, R. G., Saliman, G., & Dunn, M. F. (1980) *Biochemistry 19*, 725–731.
Parker, D. M., Hardman, M. J., Plapp, B. V., Holbrook, J. J., & Shore, J. D. (1978) *Biochem. J. 173*, 269–275.
Rafter, G. W., & Colwick, S. P. (1957) *Methods Enzymol. 3*, 887–893.
Reynolds, C. H., & McKinley-McKee, J. S. (1969) *Eur. J. Biochem. 10*, 474–478.
Reynolds, C. H., & McKinley-McKee, J. S. (1975) *Arch. Biochem. Biophys. 168*, 145–162.
Reynolds, C. H., Morris, D. L., & McKinley-McKee, J. S. (1970) *Eur. J. Biochem. 14*, 14–26.
Shore, J. D., Gutfreund, H., Brooks, R. L., Santiago, D., & Santiago, P. (1974) *Biochemistry 13*, 4185–4190.
Sigman, D. S., Frolich, M., & Anderson, R. E. (1982) *Eur. J. Biochem. 126*, 523–529.
Theorell, H., & McKinley-McKee, J. S. (1961) *Acta Chem. Scand. 15*, 1811–1833.
Winer, A. D., & Theorell, H. (1960) *Acta Chem. Scand. 14*, 1729–1742.
Zeppezauer, E., Jörnvall, H., & Ohlsson, I. (1975) *Eur. J. Biochem. 58*, 95–104.

# Kinetics of Action of Chymosin (Rennin) on Some Peptide Bonds of Bovine β-Casein†

Christophe Carles* and Bruno Ribadeau-Dumas

ABSTRACT: The first steps of proteolysis of bovine β-casein by chymosin were studied quantitatively by using reverse-phase high-performance liquid chromatography (RP-HPLC). Although chymosin has a broad specificity, it has been possible to selectively study the hydrolysis of two bonds (Ala-189–Phe-190 and Leu-192–Tyr-193) by choosing appropriate conditions. The disappearance of the substrate and the appearance of the reaction products as a function of time were followed at 220 nm by RP-HPLC. For concentrations where β-casein was in a micellar form, the Michaelian parameters corresponding to the cleavage of bond 192–193 were determined by measuring initial rates of reaction at different substrate concentrations in a time period for which splitting of bond 189–190 was negligible. The following results were obtained: $k^1_{cat} = 1.54\ s^{-1}$, $K^1_m = 0.075$ mM, and $k^1_{cat}/K^1_m = 20.6\ mM^{-1}\ s^{-1}$. Under conditions where the protein was in a monomeric state, the following parameters were determined for the splitting of bond 192–193 by integrating the Michaelis equation: $k^2_{cat} = 0.056\ s^{-1}$, $K^2_m = 0.007$ mM, and $k^2_{cat}/K^2_m = 79.7\ mM^{-1}\ s^{-1}$. Under the latter conditions the four enzymic reactions involved in the cleavage of bonds 189–190 and 192–193 were first-order reactions. The four corresponding apparent rate constants were calculated by using a computer program. Excellent agreement was obtained between concentrations of four molecular species measured during the reaction period and those calculated by using the four apparent rate constants.

Chymosin, formerly named rennin (EC 3.4.23.4), is an aspartyl proteinase of broad specificity secreted in the stomach of some newborn animals (ruminants and a few other species). Its natural protein substrates are the caseins ($\alpha_{s1}$, $\alpha_{s2}$, β, and κ) that exist in cow milk, together with inorganic ions, as high molecular weight coaggregates, the micelles. The first event that follows milk ingestion in the calf is its coagulation in the stomach. It is due to the splitting by chymosin of a single bond, Phe-105–Met-106 (Delfour et al., 1965), in κ-casein. This destroys the micelle-stabilizing properties of this protein and leads to micelle aggregation through hydrophobic interactions. Chymosin contributes to the digestion of the coagulum by a slower action on a number of peptide bonds of the four caseins. However, it has been known for a long time, from in vitro studies, that a few bonds in $\alpha_{s1}$- and β-casein are highly susceptible to chymosin.

Using gel electrophoresis, Creamer et al. (1971) observed the appearance of three bands (βI, βII, and βIII, in their order of appearance) when β-casein (209 residues) was incubated

† From the Institut National de la Recherche Agronomique, C.N.R.Z., 78350 Jouy-en-Josas, France. *Received February 27, 1984.* This work was part of a Thèse de Docteur-Ingénieur (C.C.).

* Correspondence should be addressed to this author at the University Biochemistry Group, Faculties of Medicine and Science, Division of Biochemistry, Department of Chemistry, University of Calgary, Calgary, Alberta, Canada T2N 1N4.

0006-2960/84/0423-6839$01.50/0 